

Electronic supplementary information (ESI)

Highly Conductive, Stretchable, and Breathable Epidermal Electrode Based on Hierarchically Interactive Nano-network

You Jun Fan^{‡abc}, Peng Tao Yu^{‡ac}, Fei Liang^{ac}, Xin Li^{ac}, Hua Yang Li^d, Lu Liu^{ac}, Jin Wei Cao^d, Xue Jiao Zhao^{ac},
Zhong Lin Wang^{ace}, and Guang Zhu^{acd*}

^aCAS Center for Excellence in Nanoscience, Beijing Key Laboratory of Micro-Nano Energy and Sensor, Beijing Institute of Nanoenergy and Nanosystems, Chinese Academy of Sciences, Beijing 100083, China

^bState Key Lab of New Ceramics and Fine Processing, School of Materials Science and Engineering, Tsinghua University, Beijing 100084, China

^cSchool of Nanoscience and Technology, University of Chinese Academy of Sciences, Beijing 100049, China

^dNew Materials Institute, Department of Mechanical, Materials and Manufacturing Engineering, University of Nottingham Ningbo China, Ningbo 315100, China

^eSchool of Materials Science and Engineering, Georgia Institute of Technology, Atlanta, GA 30332, United States

‡ These authors contributed equally.

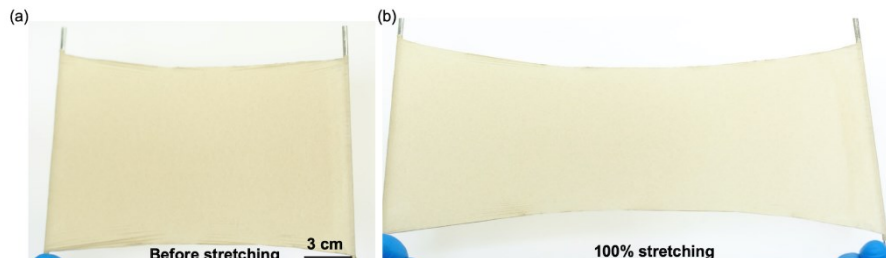


Fig. S1 (a, b) Optical camera images of the SEE film with large area before stretching and under strain of 100%.

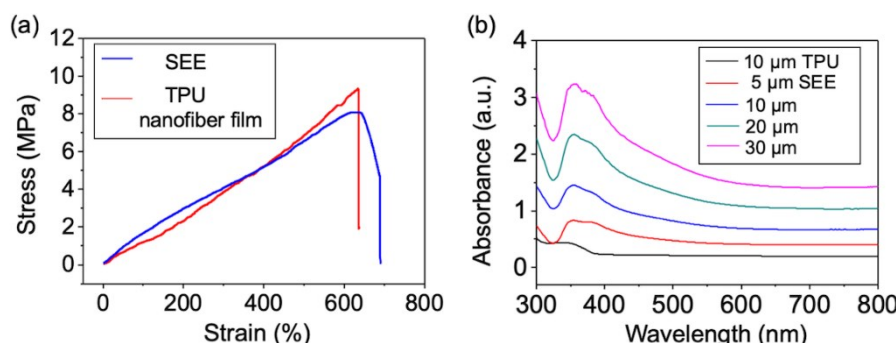


Fig. S2 (a) Stress–strain curves for the pure TPU nanofiber mat and the SEE. (b) UV-Vis absorbance spectra of the SEE with different thickness and a pure TPU nanofiber film.

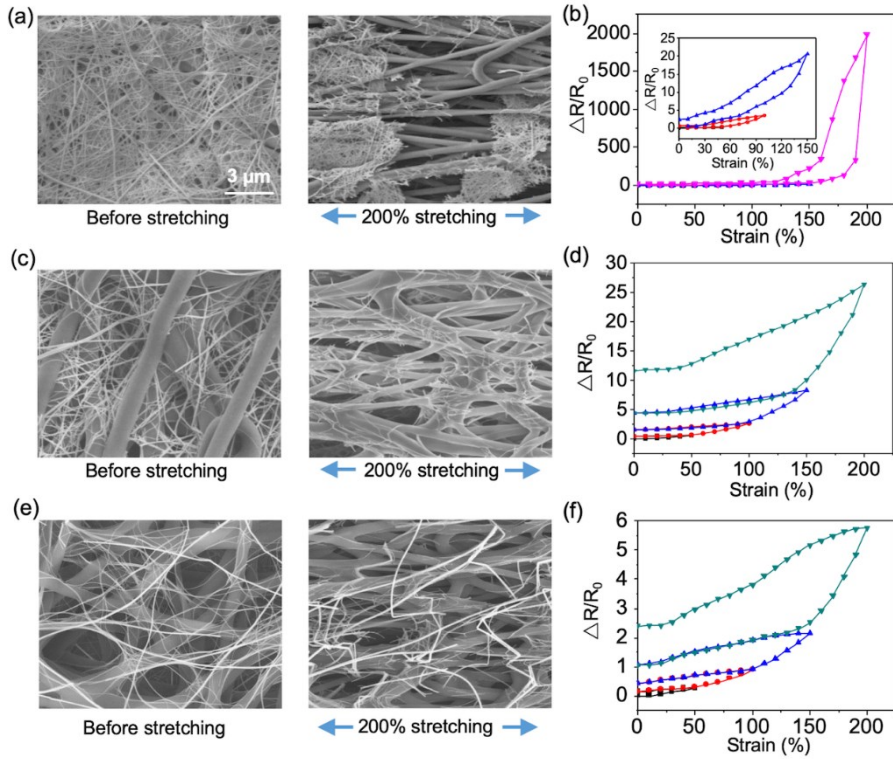


Fig. S3 SEM images of the SEE with different structures before (left) and after (right) stretching (a, c, e), and their cyclic change in resistance $\Delta R/R_0$ versus strain(b, d, f). (a) The SEE with layer by layer structure that AgNWs are deposited on TPU nanofiber mat. (c) The SEE with bonding interactive nanonetwork of TPU nanofibers and AgNWs. (e) The SEE of hierarchically interactive nanonetwork with discrete distribution of AgNWs.

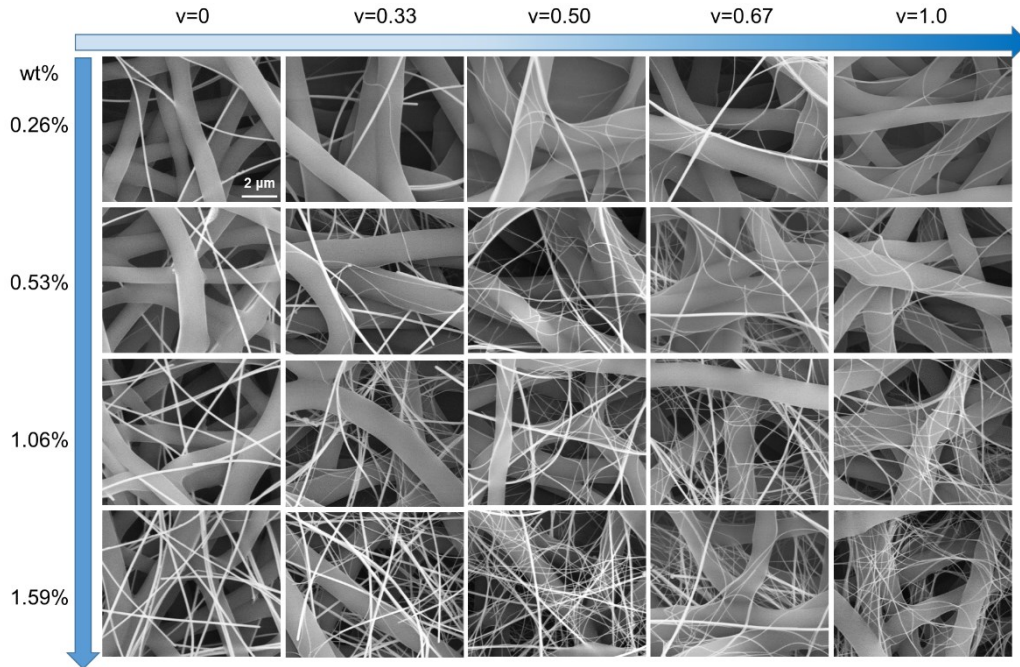


Fig. S4 SEM images of the SEE with different AgNWs contents and different component ratio of D30 and D120 AgNWs (v =Weight D30 AgNWs / Weight total AgNWs).

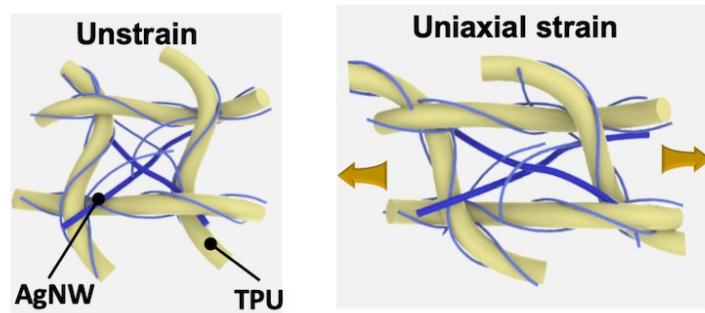


Fig. S5 Schematic diagram of the initial configuration (left) and the deformed configuration (right) at a uniaxial strain for the nano-network of the SEE.

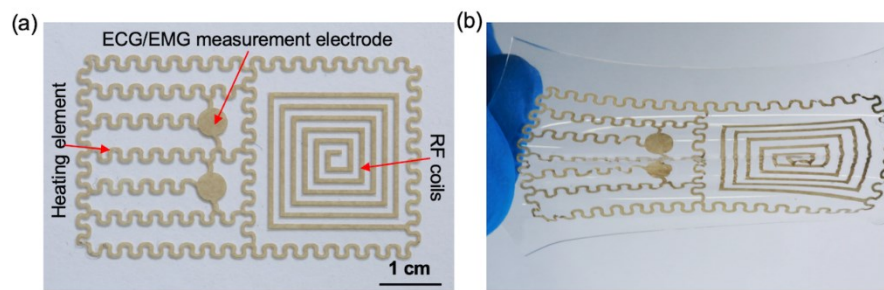


Fig. S6 Photographs of elastic circuits fabricated by SEE on a flexible PDMS film before (a) and after (b) stretching.

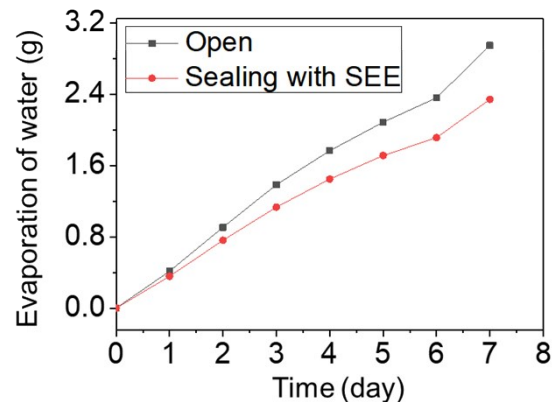


Fig. S7 Permeability property of water for the SEE, comparing with the evaporation of water in an open environment.

Table S1. The performance comparisons among AgNW-based electrodes.

Materials	Strategies	Conductivity/Sheet resistance	Stretchability	Reference
AgNWs	Roll-roll welding	Single-sided conductive, $5 \Omega \text{ sq}^{-1}$	Strain <2%	1
AgNWs on PET	Direct printed on PET	Single-sided conductive, $100 \Omega \text{ sq}^{-1}$	No stretchability	2
Ag NWs/PDMS	Composite	9.8Ω	Increase with strain up to 100%	3
Ag-MWNT/ PVDF	Composite	3100 S cm^{-2} at 8.60 wt% Ag flakes.	20 S cm^{-2} at 140% strain	4
AgNWs/PU	Layer-by-layer filtration	10000 S m^{-1}	250%	5
AgNW/dopamine-modified PDMS	Composite	$35\Omega \text{ sq}^{-1}$, at 7 wt % AgNWs.	Stable within 15%	6
Ultralong AgNWs/ Ecoflex	Transferring on a pre-strained (300%) elastomer	Single-sided conductive, $9-70 \Omega \text{ sq}^{-1}$	460%	7
PUS/AgNW/PDMS	2D/3D binary networks	$8.35-19.2 \text{ S cm}^{-1}$, AgNW mass fraction (0.5-3.3%)	Increase by 160% at 100% strain	8
Au-AgNW/ SBS	Composite, Au coated Ag NWs	41850 S cm^{-1} , at Au-AgNW weight fraction of 60%-75%	266% (max:840%)	9
3D AgNW/PDMS	2D/3D binary networks	21.5 S cm^{-1} , at AgNW density of 25 mg cm^{-3}	Increase by 150% at 100%	10
AgNW/PU	Composite	$8-44.7 \Omega \text{ sq}^{-1}$	Conductive at 60%	11
AgNW/PDMS/Zony	Composite	$4.5 \Omega \text{ sq}^{-1}$	Increase with strain up to 100%	12
AgNW/PU nanofibers	layer-by-layer	9190 S cm^{-1}	310%	13
Epoxy/NBR & AgNW/PU	Epoxy/NBR fiber spray coated with AgNW/PU nanocomposite	51Ω	less than 150Ω by stretching up to 40%	14
Muliti-level AgNWs/TPU nanofiber	Hierarchically interactive nano-network	4800 S cm^{-1} ($0.41 \Omega \text{ sq}^{-1}$), at volume fraction of 1.59%	Conductive at 500% strain	This work

Reference

- 1 S. J. Lee, Y.-H. Kim, J. K. Kim, H. Baik, J. H. Park, J. Lee, J. Nam, J. H. Park, T.-W. Lee, G.-R. Yi and J. H. Cho, *Nanoscale*, 2014, **6**, 11828-11834.
- 2 P.-H. Wang, S.-P. Chen, C.-H. Su and Y.-C. Liao, *Rsc Adv.*, 2015, **5**, 98412-98418.
- 3 C. Yan, X. Wang, M. Cui, J. Wang, W. Kang, C. Y. Foo and P. S. Lee, *Adv. Energy Mater.*, 2014, **4**, 1301396.
- 4 K.-Y. Chun, Y. Oh, J. Rho, J.-H. Ahn, Y.-J. Kim, H. R. Choi and S. Baik, *Nat. Nanotech.*, 2010, **5**, 853-857.
- 5 C. S. Boland, U. Khan, H. Benameur and J. N. Coleman, *Nanoscale*, 2017, **9**, 18507-18515.

- 6 T. Akter and W. S. Kim, *ACS Appl. Mater. Interfaces*, 2012, **4**, 1855-11859.
- 7 P. Lee, J. Lee, H. Lee, J. Yeo, S. Hong, K. H. Nam, D. Lee, S. S. Lee and S. H. Ko, *Adv. Mater*, 2012, **24**, 3326-3332.
- 8 J. Ge, H. B. Yao, X. Wang, Y. D. Ye, J. L. Wang, Z. Y. Wu, J. W. Liu, F. J. Fan, H. L. Gao, C. L. Zhang and S. H. Yu, *Angew. Chem. Int. Ed.*, 2013, **52**, 1654-1659.
- 9 S. Choi, S. I. Han, D. Jung, H. J. Hwang, C. Lim, S. Bae, O. K. Park, C. M. Tschabrunn, M. Lee, S. Y. Bae, J. W. Yu, J. H. Ryu, S.-W. Lee, K. Park, P. M. Kang, W. B. Lee, R. Nezafat, T. Hyeon and D. H. Kim, *Nat. Nanotech.*, 2018, **13**, 1048-1056.
- 10 H. L. Gao, L. Xu, F. Long, Z. Pan, Y. X. Du, Y. Lu, J. Ge and S. H. Yu, *Angew. Chem. Int. Ed.*, 2014, **53**, 4561-4566.
- 11 W. Hu, X. Niu, R. Zhao and Q. Pei, *Appl. Phys. Lett.*, 2013, **102**, 38.
- 12 J. Wang, C. Yan, W. Kang and P. S. Lee, *Nanoscale*, 2014, **6**, 10734-10739.
- 13 Z. Jiang, M. O. G. Nayeeem, K. Fukuda, S. Ding, H. Jin, T. Yokota, D. Inoue, D. Hashizume and T. Someya, *Adv. Mater.*, 2019, **31**, 1903446.
- 14 H. Y. Liu, H. C. Hsieh, J. Y. Chen, C. C. Shih, W. Y. Lee, Y. C. Chiang, W. C. Chen. *Macromol. Chem. Phys.* 2019, **220**, 1800387.